Mechanism of Electroporative Dye Uptake by Mouse B Cells

E. Neumann,* K. Toensing,* S. Kakorin,* P. Budde,# and J. Frey#
*Physical and Biophysical Chemistry and #Biochemistry II, Faculty of Chemistry, University of Bielefeld, Bielefeld, Germany

ABSTRACT The color change of electroporated intact immunoglobulin G receptor$^-$ (FcγR$^-$) mouse B cells (line IIA1.6) after direct electroporative transfer of the dye SERVA blue G (M_r 854) into the cell interior is shown to be dominantly due to diffusion of the dye after the electric field pulse. Hence the dye transport is described by Fick's first law, where, as a novelty, time-integrated flow coefficients are introduced. The chemical-kinetic analysis uses three different pore states (P) in the reaction cascade ($C \rightleftharpoons P_1 \rightleftharpoons P_2 \rightleftharpoons P_3$), to model the sigmoid kinetics of pore formation as well as the biphasic pore resealing. The rate coefficient for pore formation k_p is dependent on the external electric field strength E and pulse duration t_E. At E = 2.1 kV cm^{-1} and $t_E = 200$ μs, $k_p = (2.4 \pm 0.2) \times 10^3$ s^{-1} at $T = 293$ K; the respective (field-dependent) flow coefficient and permeability coefficient are $k_f^0 = (1.0 \pm 0.1) \times 10^{-2}$ s^{-1} and $P^0 = 2$ cm s^{-1}, respectively. The maximum value of the fractional surface area of the dye-conductive pores is 0.035 $\pm$ 0.003%, and the maximum pore number is $N_p = (1.5 \pm 0.1) \times 10^5$ per average cell. The diffusion coefficient for SERVA blue G, $D = 10^{-6}$ cm^2 s^{-1}, is slightly smaller than that of free dye diffusion, indicating transient interaction of the dye with the pore lipids during translocation. The mean radii of the three pore states are $\bar{r}(P_1) = 0.7 \pm 0.1$ nm, $\bar{r}(P_2) = 1.0 \pm 0.1$ nm, and $\bar{r}(P_3) = 1.2 \pm 0.1$ nm, respectively. The resealing rate coefficients are k_{-2} = $(4.0 \pm 0.5) \times 10^{-2}$ s^{-1} and $k_{-3} = (4.5 \pm 0.5) \times 10^{-3}$ s^{-1}, independent of E. At zero field, the equilibrium constant of the pore states (P) relative to closed membrane states (C) is $K_p^0 = [(P)]/[C] = 0.02 \pm 0.002$, indicating 2.0 $\pm$ 0.2% water associated with the lipid membrane. Finally, the results of SERVA blue G cell coloring and the new analytical framework may also serve as a guideline for the optimization of the electroporative delivery of drugs that are similar in structure to SERVA blue G, for instance, bleomycin, which has been used successfully in the new discipline of electrochemotherapy.

GLOSSARY

$\bar{a}$	mean cell radius
C	closed lipid bilayer state
c	analytical dye concentration in the bulk solution
c_o	initial analytical dye concentration in the bulk solution
D	diffusion coefficient of SERVA blue G
Dy	dye molecule
Dy^{in}	dye molecule in the cell interior
d	membrane thickness
E	effective field strength (kV cm^{-1})
E_m	transmembrane field strength
F^*	fraction of the membrane area occupied by the dye permeable pore state P_3
F_w	water percentage in the cell membrane before the field pulse
F_p^o	maximum fraction of all pore states
f	fraction of those colored cells that can potentially regenerate
f_N	renormalized fraction of colored cells
K_p, K_p^0	equilibrium constant of a dipolar transition, zero-field equilibrium constant
k_f^0	maximum flow coefficient (s^{-1})
k_f	flow coefficient (s^{-1})
k_p	rate coefficient of pore formation (s^{-1})
k_{-i}	rate coefficients of pore resealing steps (s^{-1}); i = 1, 2, 3
$\Delta_R M$	molar electric reaction dipole moment of pore formation (A s cm mol^{-1})
n_c^{in}	amount of dye in an average cell (mol)
n^{in}	total amount of dye in all cells of the suspension (mol)
n^{out}	the total amount of dye in bulk solution (mol)
N	number of colored cells
N_d	number of (colored) damaged cells before the field application
N_0	number of colored cells when dye is added before the pulsing
N_T	total number of cells
N_∞	number of colored cells at $t \rightarrow \infty$
N_p	pore number per average cell
P	electroporated lipid bilayer state
P_i	pore states during an electric pulse; i = 1, 2, 3
P_I, P_{II}	dye-permeable pore states after an electric pulse (simplified normal mode analysis)
P_2^*, P_3^*	dye-permeable pore states (after an electric pulse)
P^0	permeability coefficient (cm s^{-1}) in the absence of an external field
P^E	permeability coefficient (cm s^{-1}) in the presence of an external electric field
$\Delta_R P$	molecular electric reaction polarization of pore formation (A s cm^{-2})
r	radius of cylindrical aqueous pores with interactive dye transport
$\bar{r}_i$	mean pore radius of pore states P_i during an electric pulse; i = 1, 2, 3

Received for publication 17 July 1997 and in final form 23 September 1997.

Address reprint requests to Dr. Eberhard Neumann, Faculty of Chemistry, University of Bielefeld, P.O. Box 10 01 31, D-33501 Bielefeld, Germany. Tel.: 49-521-106-2053; Fax: 49-521-106-2981; E-mail: eberhard.neumann@post.uni-bielefeld.de.

0006-3495/98/01/98/11 $2.00

S	total surface area of electropores available for the dye transport
S_c	surface of pores per average cell
S_c^o	maximum electroporated membrane area of an average cell
S_e^{tot}	total surface area of the average cell
t_E	electric pulse duration (μs)
t_{add}	time of addition of dye to cell suspension, counted from the end of a pulse
t_{obs}	time of observation to identify the SERVA blue G-colored cells
$\Delta_R V_p$	molecular reaction volume of pore formation (cm^3)
V_c	volume of an average cell
V_o	volume of the bathing solution
z_{eff}	effective charge number (with sign) of the dye molecule

Greek symbols

β	fraction of pore state P_3*, relative to P_2* + P_3*
β_N	fraction of normal mode pore state P_I, relative to $P_I + P_{II}$
$f(\bar{\lambda}_m)$	conductivity factor
$\Delta\varphi_m$	transmembrane potential difference (V)
$\Delta\varphi_{m,s}$	saturation value of the transmembrane potential difference
$\overline{\Delta\varphi_m}$	mean electric potential difference across the electroporated membrane surface
$\bar{\lambda}_m$	angular and time average of transmembrane conductivity (S cm^{-1})
λ_i, λ_0	conductivities of the cell interior and the outside suspension, respectively
ρ_c	cell density (ml^{-1})
τ_I, τ_{II}	normal mode time constants of the resealing of P_I and P_{II} pore states, respectively

INTRODUCTION

Membrane electroporation (ME) is a powerful technique that uses electric field pulses to render cell membranes transiently porous, so that they become permeable to otherwise impermeable substances. The method is nowadays widely used to manipulate biological cells, organelles, cell aggregates, and tissue. The various applications of ME include the direct (electrophoretic) transfer of genes (Neumann et al., 1982, 1996; Neumann, 1992) and of proteins, aromatic ionic dyes (Neumann and Boldt, 1989, 1990), and drugs into the cell interior (see, e.g., Tekle et al., 1994). Recently, ME was used to improve transdermal drug delivery (Vanbever and Preat, 1995). Moreover, clinical applications of ME gain increasing importance; for instance, skin tumors can be transiently electroporated such that effective drug delivery is achieved (Heller and Gilbert, 1993; Heller et al., 1995; Sersa et al., 1995). Specifically, skin melanomas have been successfully treated by ME and low doses of bleomycin, a powerful drug that, after ME, is able to penetrate the cell interior (Heller et al., 1996; Domenge et al., 1996). Clearly, the action of bleomycin is at the level of DNA replication, where the initial step leading to cell death is the binding of bleomycin to DNA (Mir et al., 1996). Similarly, data suggest that the functionally effective step in electroporative cell transformation is the binding of the DNA to intracellular structures (Neumann et al., 1996). The electrodelivery of DNA and drugs appears to be more efficient when the permeants are first adsorbed to the outer cell surface before electrodiffusive insertion into the membrane surface and cross-membrane translocation occur. The details of the mechanism of electroporative drug transport into cells, however, are not yet well understood. Knowledge of the molecular mechanism is the basis of goal-directed strategies for optimizing the protocols for efficient electrodelivery of drugs and DNA, especially in gene therapy.

Some useful information already exists. Most instructively, the electroporative membrane transport of drug-like dyes was studied by color imaging of single cells, providing spatial and temporal resolution. Technically, one can only examine a small number of cells in a limited time. Small cell numbers may not be representative for the total populations of cells (Sowers and Lieber, 1986; Dimitrov and Sowers, 1990; Tekle et al., 1991; Hibino et al., 1993). Many other methods only yield population averages, as discussed by Kinosita and Tsong (1977, 1978) and Teissie and Tsong (1981). For instance, the number of (electro)transfected cells is only a global indicator, because after the electroporative transport of DNA across the cell membrane, successful gene expression requires cell survival and correct incorporation of the DNA into the genome of the cell. Thus gene expression itself is of only limited use in characterizing the mechanism of DNA transport through the plasma membrane.

The coloring of the electroporated cells represents a more direct access to the mechanism of the molecular transport across electroporated membranes. Here we show how cell coloring can be analyzed to yield characteristic rate parameters of the electroporation-resealing cycle in its coupling to dye transport. The data analysis leads to a variety of results that are of practical importance for the optimization of electrodelivery processes, especially in electroporative chemotherapy.

MATERIALS AND METHODS

Cell preparation

The immunoglobulin G receptor$^-$ (FcγR$^-$) mouse B cell line IIA1.6 was cultivated as described by Budde et al. (1994). The cells were washed twice with Click's medium (Biochrom KG, Berlin/Germany) without fetal calf serum and resuspended in it. The cell density was $\rho_c = 6 \times 10^6$ ml^{-1}.

SERVA Blue G

SERVA Blue G (SBG) (M_r 854), which is equivalent to Coomassie Brilliant Blue G, was obtained as a powder from SERVA Feinbiochemica

(Heidelberg, Germany). Fresh solutions of 11.7 mM SBG in serum-free Click's medium were prepared just before each experiment. SBG is an established protein dye that does not penetrate intact cell membranes (Bradford, 1976). For all electroporation experiments, the final protein dye concentration was $c_o = 1.17$ mM and $\rho_c = 6 \times 10^6$ ml^{-1}. Hence the linear cell density was ~182 cells cm^{-1}, and the mean distance between the cell centers was $d \approx 55$ μm. The IIA1.6 cells are ~25 μm in diameter; thus the average cell separation is about a cell diameter. No cell clustering was observed.

Electric field pulses

Single rectangular electric field pulses were applied with an Electroporator II (Dialog, Düsseldorf, Germany), at a voltage of up to 1 kV and with a pulse duration from 10 μs to 100 ms. This type of electroporator is particularly suited to biophysical studies of ME. The pulse shape was monitored on-line with an oscilloscope. The sample chambers (Bio-Rad, Munich, Germany) were equipped with flat parallel aluminum electrodes; the electrode distance was 0.4 cm; the maximum volume was 0.8 ml. The chambers have to be used with alternating voltage polarity to avoid major anodic oxidation of the electrodes. The counterpotentials due to galvanic electrochemical surface reactions cannot exceed 3 V, which is negligibly small compared with the initial pulse voltage $200 \leq U_0/V \leq 1000$. In this voltage range and at the low medium conductivity ($\lambda_0 = 1.3 \times 10^{-2}$ S cm^{-1}), corresponding to a low current density, the actual field strength E in the solution between the electrodes is estimated to $E = E_0 \cdot 0.85$ ($\pm$ 0.05) (Pliquett et al., 1996). To permit straightforward data analysis in terms of a defined electroporated cell surface area, the field strength $E = 0.85\ U_0/d$ was applied to the cell suspension in the form of a single rectangular pulse. Multiple pulse application is very effective for dye transfer, but as such it is not suited to the determination of important parameters such as fractional porated area or pore numbers.

Cell electroporation and counting

Membrane electroporation renders cells permeable to the dye SBG, transiently and reversibly. Depending on the field strength and the pulse duration, the blue color becomes visible within 30 min after the pulse or after the addition of the dye to the electroporated cells (Fig. 1). Almost immediately after the pulse at low field strength ($E \leq 1.5$ kV cm^{-1}, $t_E = 110$ μs), the electroporated cells exhibit blebs. The electroinduced blebs disappear within 20 min at 298 K (Gass and Chernomordik, 1990). The temperature before pulsing was $T = 295$ ($\pm$ 2) K (22 ($\pm$ 2)°C).

After pulsing 800-μl aliquots of the cell suspension, the cells were incubated for 45 min at 22 $\pm$ 2°C, and the number N of colored cells of the population was determined.

The resealing kinetics was assayed by pulsing in the absence of the dye and adding SBG at selected periods (t_{add}) after the pulse.

The colored cells were counted by using a light microscope (Olympus BH-2), video monitoring (WVP-F10E; Panasonic, Hamburg, Germany), and tape recording (NEC DX-1000G,); 6 $\times$ 100 cells (pulsed and control) were observed routinely to obtain statistically significant results. At least five replicate experiments were performed for each data point.

RESULTS

In Fig. 2 it is seen that at a given field pulse duration, the number of colored cells increases with increasing field strength. For larger pulse durations, the range of coloring is shifted to lower field strengths.

Cell coloring due to adding dye after the electroporation pulse occurs in at least two relaxation phases (Fig. 3). If N is the number of colored cells, $N_\infty = N(t_{add} \rightarrow \infty)$ represents the number of colored cells at the limiting time of administration of dye long after pulse application (Fig. 3). The fraction f of those colored cells that can potentially regenerate is defined as

$$f = (N - N_\infty)/(N_T - N_\infty) \tag{1}$$

where N_T is the total number of cells.

In the simplest form of a chemical normal mode analysis, according to Eigen and DeMaeyer (1963), this fraction may be renormalized as

$$f_N = \frac{f}{f(t_{add} = 0)} = \frac{N - N_\infty}{N_0 - N_\infty} = \beta_N \cdot e^{-t_{add}/\tau_I} + (1 - \beta_N) \cdot e^{-t_{add}/\tau_{II}} \tag{2}$$

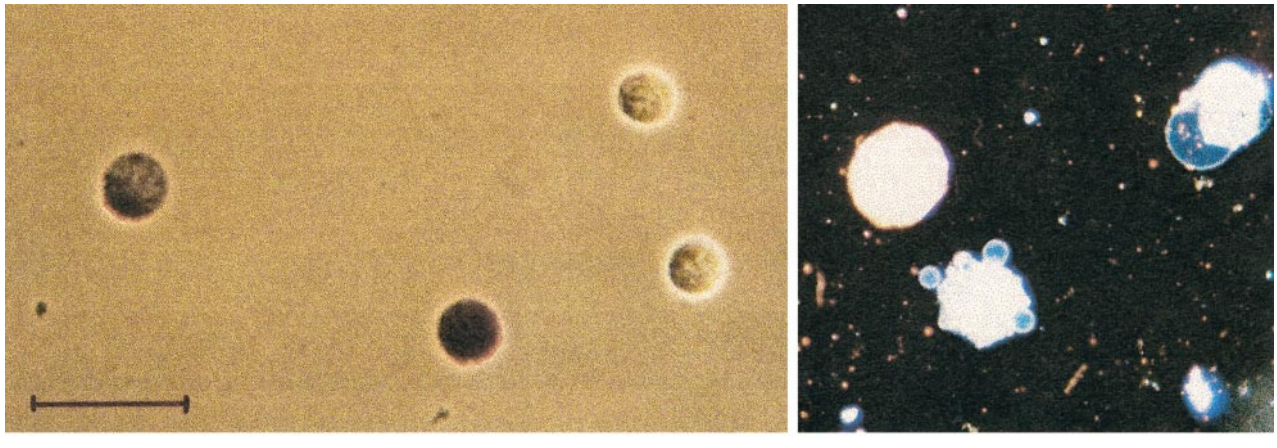

FIGURE 1 Optical image of the primary data. B-lymphoma cells (line IIA1.6) exposed to one electric field pulse ($E = 1.23$ kV cm^{-1}; pulse duration $t_E = 110$ μs) in the presence of the dye SERVA blue G (M_r 854). (*A*) Nonpermeabilized cells (*white*) and permeabilized cells (*blue*), indicated by the uptake of the dye (phase-contrast); bar = 50 μm. (*B*) Blebs are observed (dark-contrast method) almost immediately after the application of one electric pulse of low field strength ($E < E_c$).

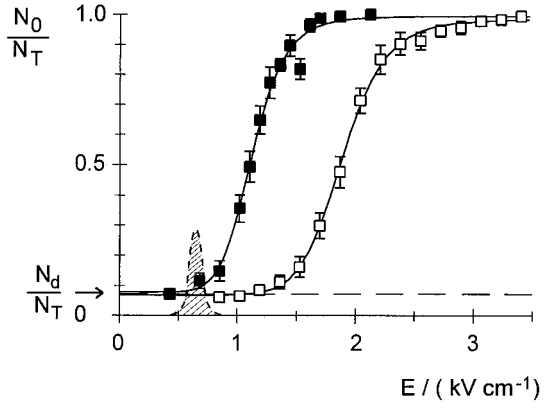

FIGURE 2 Electroporative cell coloring by the dye SERVA blue G. The fraction N_0/N_T of colored cells as a function of the external field strength E at two pulse durations $t_E/\mu s$: 50 (□) and 150 (■). N_0 is the number of blue-colored cells corresponding to the administration of SERVA blue G in the cell suspension before the pulsing, and N_T is the total number of cells. The fraction N_d/N_T at $E = 0$ (*dashed line*) represents the number of damaged cells colored before the field application. For a comparison, the range where the cells can be transfected (*shaded area*) at larger pulse durations ($t_E \approx 100$ ms) is restricted to a narrow lower field strength range (0.6–0.7 kV cm^{-1}). Experimentally, an aliquot of a suspension of mouse B-cells (line IIA1.6) was treated by one rectangular electric pulse in the presence of 1.17 mM SERVA blue G (M_r 854); the largest molecular dimension was estimated to be 2.4 ± 1 nm. CLICK's medium was based on RPMI 1640 supplemented with 10 mM Na-pyruvate, 10 mM glutamine, and 50 μM 2-mercaptoethanol. The electric conductivity of the cell suspension is $\lambda_0 = 1.3 \times 10^{-2}$ S cm^{-1}, $T = 293$ K (20°C); cell density $\rho_C = N_T/V_o \approx 6 \times 10^6$ ml^{-1}; sample volume is $V_o = 800$ μl.

where N_0 is the number of colored cells when the dye was added before the pulsing ($N_0 = N(t_{add} = 0)$); τ_I and τ_{II} are the normal mode time constants of the phases, respectively; and

$$\beta_N = [P_I]/([P_I] + [P_{II}]) \quad (3)$$

is the fraction of rapidly closing pore states, (P_I): $0 \le \beta_N \le 1$. For the case of practically unidirectional structural transitions of the resealing cascade (C ← P_I ← P_{II}), the data yield the rate coefficients $k_I = \tau_I^{-1} = 0.044$ s^{-1} and $k_{II} = \tau_{II}^{-1} = 0.003$ s^{-1} of the rapid (P_I) and at least one slowly closing pore state (P_{II}), respectively; in this example, $\beta_N = 0.63$.

The rate coefficients are practically independent of the field strength of the pulse, as expected for the resealing at $E = 0$ (data not shown). In summary, the dye uptake kinetics indicates pore resealing in at least kinetically resolved steps.

As seen in Fig. 4, the dye method can be used to explore quantitatively, in terms of $\Delta N/N_T$, the optimum field strength range for the electroporative transport of the dye or of other molecules with properties and size similar to those of the dye concerned. In all cases the range of cell loading is expected to be shifted to lower field strengths at larger pulse durations.

The linear functional dependence of the squared field strength ($E_{0.5}^2$), corresponding to the fraction $f = 0.5$ of colored cells on the reciprocal pulse duration t_E^{-1} (Fig. 5), is in line with the interfacial electric polarization mechanism of cell membrane electroporation (Neumann, 1992).

THEORY AND DATA ANALYSIS

Nernst-Planck formalism

If the permeant molecules are charged (ionic), the electroporative transport in the presence of the electroporation field naturally has an electrodiffusive component. The appropriate transport equation for small driving forces is the Nernst-Planck relationship combining Fick's first law and Ohm's first law. In the framework of a few realistic assumptions, the Nernst-Planck equation can be integrated to yield

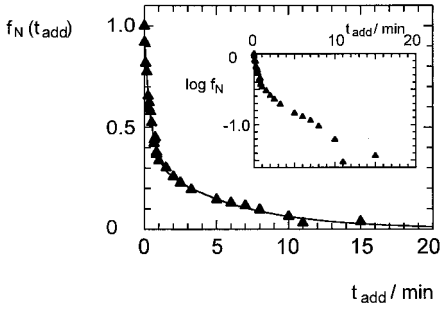

FIGURE 3 Cell resealing kinetics indicated by dye uptake. The fraction $f_N = (N - N_\infty)/(N_0 - N_\infty)$ of colored cells (Eq. 2) as a function of the time t_{add} of dye addition after the pulse of the duration $t_E = 110$ μs and the external field strength $E = 1.49$ kV cm^{-1}. (*Inset*) Semilogarithmic scale, showing the biphasic nature of the cell coloring. The initial value $f_N = 1$ for $N = N_0$ (at time $t_{add} = 0$) corresponds to the addition of the dye before the pulsing. Obviously, at $t_{add} \to \infty$, where $N = N_\infty$, $f_N = 0$. Experimental conditions were as in Fig. 2. Data were evaluated with Eq. 23 of the text.

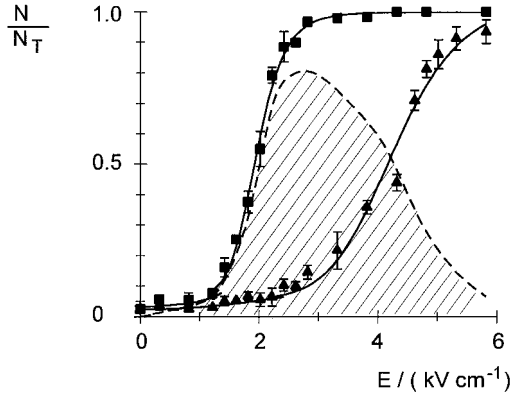

FIGURE 4 Optimal range for cell survival. The fraction N/N_T of colored cells is expressed as a function of field strength E (pulse duration: $t_E = 110$ μs). ■, N_0/N_T pulsed in the presence of dye. ▲, N_∞/N_T pulsed in the absence of dye; the dye was added 30 min after the electric pulse. Dotted line, $\Delta N/N_T = (N_0 - N_\infty)/N_T$; the shaded area represents the range of the experimental conditions of an optimal transient cell electroporation leading to transport of dyes like SERVA blue G. Experimental conditions were as in Fig. 2.

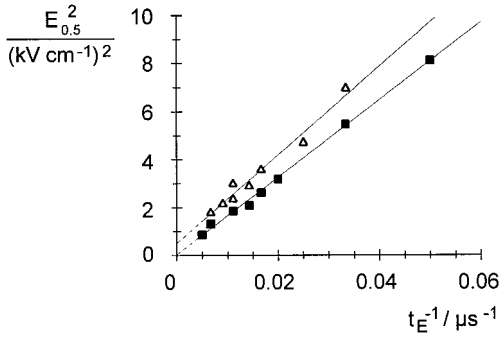

FIGURE 5 Strength-duration relationship. Square of the field strength ($E_{0.5}^2$), corresponding to the fraction $f_N = 0.5$ of colored cells (see Fig. 2), is expressed as a function of the reciprocal pulse duration ($1/t_E$) at two selected conductivities of the external medium $\lambda_0/(10^{-2}$ S cm$^{-1})$: 1.3 (■) and 1.0 (□).

the time course of the electroporative influx (or efflux) of dye molecules into (or out of) the cells (see the Appendix).

In the case of the electroporative influx of the dye SBG, the electroporated cells become colored, even if the dye is administrated a long time (minutes) after the pulse application. Therefore, Fick's part of the Nernst-Planck equation will be demonstrated to be sufficient to describe the mole flow of the dye through the electroporated cell membranes into the cell interior.

Fick's first law formalism

Even if the dye is present during the pulse, the blue color of electroporated cells only becomes visible at times t_{obs} that are much larger (≥5 min) than the pulse duration t_E (100 μs), indicating that the dye-permeable pore states are long-lived, as already indicated by the slow resealing kinetics (Fig. 3). Because $\tau_I = 23$ s and $\tau_{II} = 327$ s, the data suggest that the main dye uptake occurs at times $t \gg t_E$, i.e., after the pulse termination (at $E = 0$).

Apparently, a few seconds after the electric pulse, the cell membrane is still so permeable that the main dye uptake, leading to coloring, takes place in the post-field time interval (Neumann et al., 1982; Neumann and Boldt, 1989). In fact, when we analyze Fig. 3, we see that the dye uptake is practically the same whether the probes were added before or a few seconds after the electric pulse. Therefore, even though the electrodiffusive dye flow through the pores in the presence of the field is many times larger than the flow without the field, the increase in the amount n^{in} of substance dye within the cells during the short pulse duration ($t_E \leq 200$ μs) is significantly smaller than that in the long time (t_{obs}) after pulse termination. The dye uptake, leading to the effective coloring of the cells, is basically an after-field effect (like that of DNA; Neumann et al., 1982), and may therefore be considered as diffusion of the dye through long-lived electroporated membrane patches. Nevertheless, the field-on time interval (t_E) is crucial for the extent of the dye uptake after the pulse, because the external field is causative in the creation of the long-lived pore states.

The cell ensemble kinetics of cell coloring may be represented as the progressive color increase in one average cell. The facilitated diffusion of the dye through the electroporated membrane patches is viewed as an interactive migration, via transient contacts of the dye with the lipids of the pore edges. The key of our analysis, in terms of Fick's first law, is that the flow coefficient k_f contains a time-dependent pore surface term. The unidirectional mole flux vector for the increase n_c^{in} in the amount of dye in the average cell is given by

$$\frac{dn_c^{in}}{dt \cdot S_c(t)} = -D \cdot \frac{dc}{dx} \tag{4}$$

where $S_c = N_p \pi r^2$ is the surface area of the N_p cylindrical aqueous pores of pore radius r with interactive dye transport in the average cell, and D is the diffusion coefficient of the dye molecules interactively permeating along the x axis through the porated patches. Conventionally, the concentration gradient of the dye influx in the x direction into the cell is approximated by the linear form

$$dc/dx = (c^{in} - c)/d \tag{5}$$

where d is the membrane thickness; $c^{in} = n_c^{in}/V_c$ is the concentration of dye in the cell; V_c is the average cell volume; c is the analytical dye concentration in the bulk solution: $c = c_o - (N\, n_c^{in}/V_o)$, where c_o is the initial analytical dye concentration in the bulk solution; and V_o is the volume of the bathing solution. Because $V_c = 4\pi\bar{a}^3 = 8.2 \times 10^{-9}$ cm^3, where $\bar{a}$ is the mean cell radius, $V_o \approx 0.76$ cm^3, and $N_T = \rho_c \cdot V_o \approx 4.8 \times 10^6$, we see that $V_o \gg N_T \cdot V_c$. We therefore may use the approximation $dc/dx = (n_c^{in}/V_c - c_o)/d$. Substitution into Eq. 4 yields the experimentally handy flux equation

$$\frac{dn_c^{in}}{dt \cdot S_c(t)} = \frac{D}{d}(c_o - n_c^{in}/V_c) \tag{6}$$

The dye uptake is given by integration of Eq. 6 in the postfield time interval as

$$n_c^{in} = c_o \cdot V_c \cdot \left(1 - \exp\left(-\frac{D}{V_c \cdot d} \cdot \int_{t_0}^{t_{obs}} S_c(t)dt\right)\right) \tag{7}$$

where $t_0 = t_E \approx 0$, if the dye is added to the cell suspension before the pulse, or, alternatively, $t_0 = t_{add}$, if the dye is added after the pulse. As the characteristic times of pore resealing ($\tau_I = 23$ s and $\tau_{II} = 327$ s) are much shorter than the time of observation ($t_{obs} \approx 1800$ s), we may set $t_{obs} \approx \infty$.

The influx ceases, even if the pores stay open, when the concentration equality $n_c^{in}/V_c = c \approx c_o$ is reached. For this limiting case, the generalization of the coloring process of one average cell to the whole ensemble of cells yields a fraction f of the colored cells equal to unity (see Eq. 1).

Generally, we have

$$f(t_E, t_{add}) \approx \frac{n_c^{in}(t_E, t_{add})}{c_o \cdot V_c} = 1 - \exp\left(-\frac{D}{V_c \cdot d} \cdot \int_{t_0}^{t_{obs}} S_c(t)dt\right) \quad (8)$$

In further analysis $S_c(t)$ is explicitly specified by Eq. A12 (see Appendix).

Membrane electroporation and dye transport

The $f(t_E)$ data in Fig. 6 confirm, in terms of the quantitative model, that the dye adsorption on the cell surface and the dye transport through the membrane are coupled to electroporated membrane states. The actual cross-membrane transport of dye molecules (Dy) through the electropores (P), being an interactive diffusional process, does not require the presence of an external field. Chemically, the coupling of the dye binding to the electroporation state transition (C $\rightleftharpoons$ P), where C is the closed membrane state, is modeled by the scheme

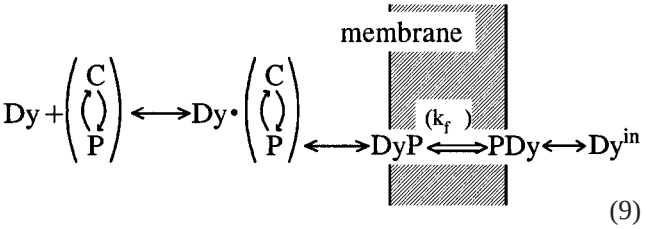

(9)

where Dy and Dy^{in} symbolize the dye in the bathing solution and in the cell interior, respectively, and the step DyP $\Leftrightarrow$ PDy models the actual translocation process. Here the flow coefficient k_f is given by

$$k_f = DS_c/(V_c d) \quad (10)$$

Because the bulk dye concentration is relatively high, the dye adsorption in Scheme 9 may be considered as a pseudo-first-order binding reaction, such that the dye concentration c appears as a constant in the expressions for the rate coefficients.

The description of the data in Figs. 3 and 6 in terms of the electroporation-resealing cycle requires an extension of the simple electroporation scheme C $\rightleftharpoons$ P (Neumann and Boldt, 1989). The rather long sigmoid phase of $f(t_E)$ (Fig. 6) suggests that there are at least three pore states P_i, $i = 1, 2, 3$, respectively. In the scheme

$$C \underset{k_{-1}}{\overset{k_1}{\rightleftharpoons}} P_1 \underset{k_{-2}}{\overset{k_2}{\rightleftharpoons}} P_2 \underset{k_{-3}}{\overset{k_3}{\rightleftharpoons}} P_3 \quad (11)$$

the states P_1 and P_2 denote pore structures of negligibly small permeability for the dye during the pulse time t_E. Only the state P_3 is required to have a finite permeability for the dye molecules. Pore resealing is described by the reverse reaction steps with the rate coefficients k_{-i}. If in the presence of the external field pore resealing can be neglected, the unidirectional reaction sequence C $\rightarrow P_1 \rightarrow P_2 \rightarrow P_3$ with the rate coefficients k_i applies.

Presence of dye during the field pulse

The penetration of the dye through electroporated membrane patches is most likely not free diffusion through large aqueous pores. Rather, it appears that the diffusion, although facilitated through electroporation, is partially "hindered" by interaction of the dye with the edge lipids of the pore states P, leading to a smaller diffusion coefficient compared with free diffusion. The concept of interactive diffusion, characterized by short-lived contacts between the lipids of the pore wall and the dye, is also useful for describing the observed specificity of transport of charged dyes, even against the electric field direction, as observed by Tekle et al. (1994).

In our case the interactive transport may be described in terms of transient complexes Dy · P between dye and pore edge lipids, formed unidirectionally through electroporation:

$$C \overset{k_p}{\rightarrow} P_1 \cdot Dy \overset{k_p}{\rightarrow} P_2 \cdot Dy \overset{k_p}{\rightarrow} P_3 \cdot Dy \rightarrow \ldots \quad (12)$$

where, for simplicity, all of the electroporation rate coefficients $k_1 = k_2 = k_3 = k_p$ are equal. The equality of the coefficients k_p means that the transitions between the pore states are associated with equal reaction volumes ($\Delta_R V_p$) of interfacial pore polarization. This assumption is theoretically justified by the corresponding minima in the hydrophobic force profiles as a function of distance from the lipid walls (Israelachvili and Pashley, 1984). As discussed previously, the data are consistent with the cooperative transi-

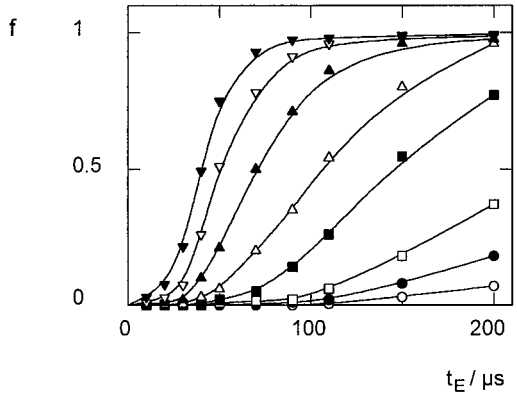

FIGURE 6 Kinetics of membrane electroporation. Fraction $f = (N - N_\infty)/(N_T - N_\infty)$ of those colored cells that can potentially regenerate (Eq. 1) as a function of the pulse duration t_E at various external field strengths E/kV cm^{-1}: ○, 0.64; ●, 0.85; □, 1.06; ■, 1.28; △, 1.49; ▲, 1.7; ▽, 1.91; ▼, 2.13; respectively. Solid lines reflect the theoretical analysis of the data with Eq. 24. Other experimental conditions were as in Fig. 2.

tion of a lipid cluster L_n forming a pore with, on average, n lipid molecules in the pore edge. For the reaction step $(i-1) \rightleftharpoons i$ such a transition is electrothermodynamically described by a (molar) cluster transition dipole moment $\Delta_R M = M_i - M_{i-1}$ and in terms of volume polarization:

$$\Delta_R M = \Delta_R V_p \cdot N_A \cdot \Delta_R P \tag{13}$$

where N_A is the Avogadro constant. For cylindrical cross-membrane pores, $\Delta_R V_p = \pi \cdot d \cdot (\langle r_i^2 \rangle - \langle r_{i-1}^2 \rangle)$ is the average aqueous pore volume change ($i = 1, 2, 3$; note that $\langle r_0^2 \rangle = 0$); $\Delta_R P$ is the reaction polarization, i.e., the difference in the polarization between pore internal water and the polarization of the same volume filled with lipids: $\Delta_R P = \epsilon_0 \cdot (\epsilon_w - \epsilon_L) \cdot E_m$, where ϵ_0 is the vacuum permittivity, and $\epsilon_w \approx 80$ and $\epsilon_L \approx 2$ are the dielectric constants of water and of lipids, respectively. E_m is the transmembrane field strength, defined according to Maxwell as negative electric potential gradient. Here $E_m = -\Delta\varphi_m/d$.

The average pore radius for a pore state P_i is defined as

$$\bar{r}_i = (i \cdot \Delta_R V_p/(\pi \cdot d))^{1/2} = \bar{r}_1 \cdot i^{1/2} \tag{14}$$

The electric field dependence of the equilibrium constant $K_p = k_p/k_{-p}$ of a dipolar transition is generally described by (see, e.g., Schwarz, 1967; Neumann, 1989)

$$K_p(E) = K_p(0) \cdot e^x \tag{15}$$

where $K_p(0)$ refers to $E = 0$. Note that $K_p(0)$ contains physical parameters such as eventual surface tension and field-dependent area-difference elastic energy terms (Evans, 1974) or area-difference elasticity (ADE) energy (Seifert and Lipowsky, 1995). In the integration boundaries $E = 0$ and $E = E_m$ we obtain (Neumann and Kakorin, 1996)

$$X = \frac{\int_0^{E_m} \Delta_R M \, dE_m}{R \cdot T} \tag{16}$$

where E_m is the actual effective force on the charged and dipolar membrane components (Neumann, 1996).

The dye-permeable pores are dominantly present in the pole caps of the cells (see, e.g., Tekle et al., 1991). Insertion of Eq. 13 into Eq. 16 yields the field factor X (Kakorin et al., 1996):

$$X \approx \frac{9 \cdot \Delta_R V_p \cdot \bar{a}^2 \cdot \epsilon_0 \cdot (\epsilon_w - \epsilon_L)}{8 \cdot k_B \cdot T \cdot d^2} \cdot f^2(\bar{\lambda}_m) \cdot E^2 \tag{17}$$

where E is the external field strength, $\bar{a}$ is the mean cell radius, and $f(\bar{\lambda}_m)$ is the conductivity factor describing the changes in the average conductivity $\bar{\lambda}_m$ of the membrane with the field strength; see Eq. A5 of the Appendix.

Transport of dye added after electroporation

The simplified normal mode analysis of the data in Fig. 3 already shows that at least two relaxation modes with significantly different time constants can be discerned. The rate of transient pore formation in the absence of an external field is probably much smaller than that of the respective pore resealing process. Therefore, a unidirectional scheme is adequate for the coupling of pore resealing with dye transport in terms of two permeable interactive dye-pore complexes, $P_2^* \cdot Dy$ and $P_3^* \cdot Dy$, according to

$$C \underset{k_{-1}}{\longleftarrow} P_1 \cdot Dy \underset{k_{-2}}{\longleftarrow} P_2^* \cdot Dy \underset{k_{-3}}{\longleftarrow} P_3^* \cdot Dy \tag{18}$$

The two resealing rate coefficients k_{-2} and k_{-3} describe the zero-field decay of dye-permeable pore states P_2^* and P_3^*. Apparently $k_{-3} \gg k_{-2}$; thus the two resealing modes are considered as independent, and the resealing kinetics of the dye-permeable membrane area S_c is described by

$$S_c(t) = S_c(t_E) \cdot \{\beta \cdot e^{-k_{-3} \cdot t} + (1-\beta) \cdot e^{-k_{-2} \cdot t}\} \tag{19}$$

where $\beta = [P_3^*]/([P_2^*] + [P_3^*])$ is the fraction of dye-interactive pore states.

We now combine Eq. 8 with Eq. A12 (see Appendix) and Eq. 19 and integrate. The dye uptake is then described by the cell fraction for a given pulse duration t_E and a given time of dye addition after the pulse:

$$f(t_E, t_{add}) = 1 - \exp\{-A(k_f^0, k_p, t_E) \cdot B(\beta, k_{-2}, k_{-3}, t_{add})\} \tag{20}$$

where

$$A = k_f^0 \cdot \left[1 - \left(1 + k_p \cdot t_E \cdot \left(1 + \frac{k_p \cdot t_E}{2}\right)\right) \cdot e^{-k \cdot t_E}\right] \tag{21}$$

$$B = \frac{\beta}{k_{-3}} \cdot e^{-k_{-3} \cdot t_{add}} + \frac{1-\beta}{k_{-2}} \cdot e^{-k_{-2} \cdot t_{add}} \tag{22}$$

In Eq. 20, k_f^0 is the maximum flow coefficient ($k_f^0 = DS_c^o/V_c d$) and S_c^o is the maximum electroporated membrane area of the average cell. If the exponential term $A \cdot B$ in Eq. 20 is smaller than unity, Eq. 20 takes the form $f \approx A \cdot B$, which is typical for a normal mode analysis for small perturbations (see Eq. 2), yet with physically specified preexponential coefficients,

$$f(t_E, t_{add}) \approx k_f^0 \cdot \left[1 - \left(1 + k_p \cdot t_E \cdot \left(1 + \frac{k_p \cdot t_E}{2}\right)\right) \cdot e^{-k_p \cdot t_E}\right] \cdot \left[\frac{\beta}{k_{-3}} \cdot e^{-k_{-3} \cdot t_{add}} + \frac{1-\beta}{k_{-2}} \cdot e^{-k_{-2} \cdot t_{add}}\right] \tag{23}$$

Note that here β/k_{-3} and $(1-\beta)/k_{-2}$ correspond to β_N and $(1-\beta_N)$, respectively, of the conventional simplified normal mode analysis (Eq. 2). The data in Fig. 3 are evaluated with Eq. 23. The data in Fig. 6 are analyzed with

$$f(t_E) \approx k_f^0 \cdot \left[1 - \left(1 + k_p \cdot t_E \cdot \left(1 + \frac{k_p \cdot t_E}{2}\right)\right) \cdot e^{-k_p \cdot t_E}\right] \tag{24}$$

which is the explicit form of Eq. A9 with Eq. A12.

DISCUSSION

Previously, electroosmosis has been suggested by Dimitrov and Sowers (1990) as a possible mechanism for the efflux of fluorescent dyes induced by exponentially decaying electric pulses in erythrocyte ghosts. The results of membrane electroporation of National Institutes of Health 3T3 cells revealed that after-field diffusion is the most probable process for the cellular uptake of foreign molecules as compared with electroosmosis or electrophoresis (Tekle et al., 1990, 1991, 1994). Alternatively, the long-lived fusogenic membrane state without electropores and probable cell fusion (Sowers, 1987; Montane et al., 1990) cannot be responsible for the dye uptake dominantly occurring after the pulse termination. Actually, the micrographs of the electroporated B cells (Fig. 1) show no cell aggregates or fusionates at the pulse durations and field strengths applied in our experiment. In line with Tekle et al. (1990, 1994), our observations suggest that post-field diffusion is the dominant mechanism of electroporative dye transport across the B cell membrane.

As expected for $E = 0$, the values of the resealing rate coefficients $k_{-3} = (4.0 \pm 0.5) \times 10^{-2}\ s^{-1}$ and $k_{-2} = (4.5 \pm 0.5) \times 10^{-3}\ s^{-1}$ and the maximum flow coefficient $k_f^0 = DS_c^o/V_c d = (1.0 \pm 0.1) \times 10^{-2}\ s^{-1}$ are practically independent of the electric field (data not shown). If we assume that because of the transient interactions between pore edge lipids and dye the diffusion coefficient of SBG in the pores is only $D = 10^{-6}\ cm^2\ s^{-1}$, compared with the estimated value for free diffusion $D_o \approx 5 \times 10^{-6}\ cm^2\ s^{-1}$, then for $d = 5$ nm we obtain the membrane permeability coefficient for the dyes $P^0 = D/d = 2\ cm\ s^{-1}$. Hence the maximum porated area in the cell membrane is $S_c^o = k_f^0 V_c/P^0 = (4.1 \pm 0.5) \times 10^{-7}\ cm^2$. As the total cell surface area is $S_c^{tot} = 2 \times 10^{-5}\ cm^2$, the maximum fraction $F_p^o = (S_c^o/S_c^{tot})$ of all pore states ($P_1 + P_2 + P_3$) amounts to the rather small value of 0.021 ± 0.002, or $2.1 \pm 0.2\%$.

The fraction β of P_3^* pores is changing with the field strength $0.42 \le E/kV\ cm^{-1} \le 2.1$ in the range $1 \le \beta \le 0.948$. For the range where $(1 - \beta) \ll \beta$, the equilibrium constant K_p for the reaction scheme $C \rightleftharpoons P$ can be calculated as $K_p \approx k_p/k_{-3}$. At field strengths up to $E = 2.1\ kV\ cm^{-1}$, the equilibrium constant K_p changes enormously in the range $2 \times 10^{-2} \le K_p \le 6 \times 10^4$ (Fig. 7). The analysis of the linear part of $\ln K_p(E^2)$ in this low field interval (Fig. 7) according to the reaction sequence in Eq. 12 and applying Eqs. 15 and 17 yields the zero-field equilibrium constant $K_p^0 = (2.0 \pm 0.2) \times 10^{-2}$ and the reaction pore volume $\Delta_R V_p = (9 \pm 1) \times 10^{-26}\ cm^3$ for the structural transitions. By substitution of $\Delta_R V_p$ in Eq. 14, we obtain the (interactive) mean pore radii: $\bar{r}_1 = 0.7 \pm 0.1$ nm, $\bar{r}_2 = 1.0 \pm 0.1$, and $\bar{r}_3 = 1.2 \pm 0.1$ nm of the P_1, P_2, and P_3 pore states, respectively. The associated numbers of lipids in the pore edge clusters in the two membrane leaflets of the bilayer are 18, 24, and 26, respectively. The value of $K_p^0 = 0.02$ is eventually overestimated, because it might contain the finite terms of the surface tension and the area-difference elastic energy (Evans, 1974; Neumann and Kakorin, 1996). Thus the magnitude of the constant $K_p^0 = 0.02$ gives the upper limit of the small percentage F_w of water in the cell membrane before the field pulse: $F_w \le 0.02$, or $\le 2\%$, in line with conventional estimates of the membrane water volume content of 9–21% in the head-group region of egg yolk phosphatidylcholine lipids in the liquid crystalline phase (McIntosh and Magid, 1993) and the suggestion that there is only 1.0–2.0% water in the hydrocarbon region of the cell membrane.

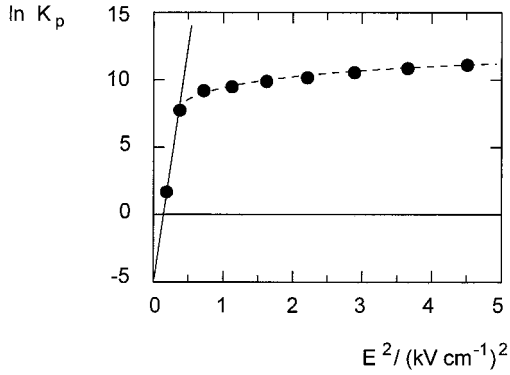

FIGURE 7 Logarithm of $K_p = [P]/[C]$ of the overall state transition $C \rightleftharpoons P$ as a function of the square of the field strength. The solid straight line indicates the theoretically predicted linear increase in $\ln (K_p(E^2))$ at a constant transmembrane conductivity. The saturation is caused by the increase in number and size of conductive pores. The increased transmembrane conductivity prevents further charging of the cell membrane.

The SBG molecule may be roughly modeled as an elongated parallelepiped of dimensions of 2.4 nm × 1.4 nm × 0.2 nm. The diameter (2.4 nm) of the pore state P_3 equals the long axis (2.4 nm) of SBG. We presume, however, that the dye molecules most likely pass the membrane oriented with the long axis along the membrane normal.

The mean pore radius $\bar{r}_3$ of the pore state P_3 is in line with previous estimates (Weaver and Chizmadzhev, 1996). However, $\bar{r}_3 = 1.2$ nm seems to be rather large. An open pore of this size should lead to a locally significant transmembrane conductivity, reducing the local transmembrane voltage (Kakorin et al., 1996), eventually causing leakage of cell components and, finally, cell death. Note, however, that the detection of the pore state P_3 (as well as P_2^* and P_3^* after the field pulse) is only possible when the SBG molecules are (interactively) passing through the pore. Therefore, the P_3 pore state is temporarily blocked by the dye molecule, reducing the average conductivity compared with a dye-free pore of the same radius. The saturation value of the transmembrane potential difference of the electroporated B cell membrane is calculated to be $\Delta\varphi_{m,s} = -0.7 \pm 0.1$ V. The value $\Delta\varphi_{m,s} = -0.7$ V is typical of that estimated for the most cell membranes by Weaver and Chizmadzhev (1996) and does not suggest any extraordinarily high local transmembrane conductivity.

According to Eq. A12, the fraction of the area occupied by the dye-permeable pores P_3 is given by

$$F^*(t_E) = \frac{S(t_E)}{S_c} = F_p^o \cdot \left[1 - \left(1 + k_p \cdot t_E \cdot \left(1 + \frac{k_p \cdot t_E}{2}\right)\right) \cdot e^{-k_p \cdot t_E}\right] \quad (25)$$

At $E = 2.1$ kV cm^{-1} and $t_E = 200$ μs, we obtain $F^* = 3.5 \times 10^{-4}$, or $0.035 \pm 0.003\%$, which is rather small. This corresponds to $N_p = (1.5 \pm 0.1) \times 10^5$ pores per average cell. The small numbers rationalize the rather slow transmembrane flow of the dye molecules leading to cell coloring. The fraction F^* compares well with the value $2 \times 10^{-3} < F < 2 \times 10^{-4}$ of conductive electropores in sea urchin eggs under approximately the same experimental conditions, derived from fluorescence imaging data by Hibino et al. (1993).

CONCLUSION

The coloring of the electroporated cells has been shown to be a useful tool for the study of the kinetics of electric pore formation and resealing as well as the transport of dye molecules through the porous membrane patches. The main results are the following:

1. A minimum number of three different pore states is required for the electroporation/resealing cycle of mouse B cells, governing the characteristic pronounced sigmoid onset in the kinetics of the cell coloring.

2. Efficient (visible) dye uptake only takes place during the long time interval after the short pulse duration, where the dye uptake into the electroporated cells is probably an interactive (and not completely free) diffusion of the dye across the electroporated membrane.

3. The results of our analysis of the electroporative dye transport may serve as a quantitative basis for optimization strategies to improve the conditions for drug delivery by membrane electroporation, such as in electrochemotherapy. One specific procedural aspect is the longevity of the porous membrane states, such that the main drug delivery should be experimentally arranged for the long-lasting resealing phase. Furthermore, local cooling should speed up the drug influx because low temperatures slow down the resealing processes.

APPENDIX

Nernst-Planck transport relationship

In the general case, the electrodiffusive mole flow density vector of the amount (n_c^{in}) of (ionic) dye molecules in the direction of the external field E into the average cell across the electroporated membrane is given by the Nernst-Planck equation in the form (Neumann et al., 1996)

$$\frac{dn_c^{in}}{S_c \cdot dt} = -\frac{D}{d}\left[\frac{n_c^{in}}{V_c} - \frac{n^{out}}{V_o}\left(1 - \frac{|z_{eff}| \cdot e_0}{k_B \cdot T}\overline{\Delta\varphi_m}\right)\right] \quad (A1)$$

where S_c is the surface area of all N_p pores of the average cell and V_c is the volume of the average cell; d is the membrane thickness; D is the effective diffusion coefficient of the dye across the electroporated surface patches (in interactive contact with dye); $|z_{eff}|$ is the absolute value of the effective charge number (with sign) of the dye molecule; e_0 is the elementary charge; k_B is the Boltzmann constant; T is the absolute temperature; $\bar{\Delta}\varphi_m$ is the mean electrical potential difference across the electroporated membrane surface; n^{out} is the total amount of dye; and V_o is the volume of the bulk solution.

By spatial integration of the dye concentration within the membrane phase, analogous to the treatment by Hodgkin and Katz (1949), we obtain

$$\frac{dn_c^{in}}{dt \cdot S_c} = -P^0 \cdot |z_{eff}| \cdot u \cdot \frac{c_o \cdot e^{-|z_{eff}| \cdot u} - c^{in}}{e^{-|z_{eff}| \cdot u} - 1} \quad (A2)$$

where $c_o = n^{out}/V_o$, $c^{in} = n_c^{in}/V_c$ and $P^0 = \gamma D/d$ is the conventional permeability coefficient (m s^{-1}), γ is the partition coefficient of dye molecules between bulk water and aqueous pore volume, and $u = F \cdot \overline{\Delta\varphi}/(RT)$ is the electric factor, where F is the Faraday constant and $R = k_B \cdot N_A$ is the gas constant. Because the SBG molecule is an anion, the electrodiffusive part of the transport caused by one DC pulse refers to only one hemisphere of the average cell. Therefore the average potential difference term operative for the dye-anion flux is defined by

$$\overline{\Delta\varphi_m} = \frac{1}{2}\int_0^{\pi/2} \Delta\varphi_m(\theta)\sin\theta\, d\theta = -\frac{3}{8}\bar{a}\, E \cdot f(\bar{\lambda}_m) \quad (A3)$$

where $\Delta\varphi_m(\theta) = -\frac{3}{2}\bar{a}E \cdot f(\bar{\lambda}_m) \cdot |\cos\theta|$, θ is the azimuthal angle with respect to the external field direction in the polar coordinate system of the cell, and $\bar{a}$ is the mean cell radius; here $\bar{a} = 12.5$ μm. The conductivity factor $f(\bar{\lambda}_m)$, describing the changes in the membrane conductivity during the electroporation process, is given by (e.g., Neumann, 1989)

$$f(\theta, \lambda_m) = 1/(1 + \bar{\lambda}_m \cdot (2 + \lambda_i/\lambda_0)/(2 \cdot \lambda_i \cdot d/\bar{a})) \quad (A4)$$

where λ_i, λ_0 are the conductivities of cell interior and the outside suspension, respectively, and $\bar{\lambda}_m$ is the angular and time average of the membrane conductivity (Kakorin et al., 1996):

$$\bar{\lambda}_m = \frac{1}{2 \cdot t_E} \cdot \int_0^{t_E}\int_0^{\pi} \lambda_m(\theta, t) \cdot \sin\theta\, d\theta\, dt \quad (A5)$$

Presence of dye before the pulsing

Generally, the dye uptake may be subdivided into two time intervals: *the field-on time interval* $0 \le t \le t_E$, where dye electrodiffusion dominates over the passive diffusion, characterizable by the permeability coefficient $P^E = P^0 \cdot (1 + |z_{eff}| \cdot F \cdot \overline{\Delta\varphi_m}/(RT)) \gg P^0$) (Neumann et al., 1996), and *the field-off time interval* $t_E \le t \le t_{obs}$, characterized by the passive dye diffusion. If $|\overline{\Delta\varphi_m}| \gg 25$ mV, as in the case in this study, the fraction of total dye uptake is obtained by integration of Eq. A2 in these two time intervals:

$$f = \frac{n_c^{in}}{c_o \cdot V_c} = \frac{n^{in}}{c_o \cdot V_c \cdot N} = \mathbf{W}(t_E) + \mathbf{Z}(t_{obs}) \quad (A6)$$

where

$$\mathbf{W} = \frac{\exp(-|z_{\text{eff}}| \cdot u)}{\exp(-|z_{\text{eff}}| \cdot u) \cdot \dfrac{N \cdot V_c}{V_o} + 1} \times \left[1 - \exp\left(-P^0 \cdot \frac{-|z_{\text{eff}}| \cdot u}{\exp(-|z_{\text{eff}}| \cdot u) - 1} \cdot \left(\frac{\exp(-|z_{\text{eff}}| \cdot u)}{V_o} + \frac{1}{N \cdot V_c}\right) \cdot \int_0^{t_E} S(t)\mathrm{d}t\right)\right] \quad \text{(A7)}$$

$$\mathbf{Z} = \frac{1}{1 + \dfrac{V_c \cdot N}{V_c}} \cdot \left(1 - \exp\left(-P^0 \cdot \left(\frac{1}{V_o} + \frac{1}{N \cdot V_c}\right) \cdot \int_{t_E}^{t_{obs}} S(t)\mathrm{d}t\right)\right)$$

In Eq. A7 V_o is the total volume of the extracellular solution, $c_o = 1.17$ mol $\cdot$ m^{-3} is the analytical dye concentration in the bulk solution, and $S = N \cdot S_c$ is the total pore surface area of all N cells available for the dye transport during and after the field pulse. If the characteristic time of pore resealing is much shorter than the time of observation, the analytical approximation $t_{obs} \rightarrow \infty$ applies in Eq. A7. As outlined in detail in the text, the main dye uptake takes place in the post-field time interval. Therefore the term W in Eqs. A6 and A7 can be neglected such that $f = Z(t_{obs})$. Provided that $V_o \gg N \cdot V_c$, which is usually the case, Eq. A6 simplifies to

$$f(t_E) \approx 1 - \exp\left\{-\frac{P^0}{N \cdot V_c} \cdot \int_{t_0}^{t_{obs}} S(t_E, t) \cdot \mathrm{d}t\right\} = 1 - \exp\left\{-\frac{P^0}{V_c} \cdot \int_{t_0}^{t_{obs}} S_c(t_E, t) \cdot \mathrm{d}t\right\} \quad \text{(A8)}$$

where $t_0 = t_E \approx 0$, if the dye is added to the cell suspension before the pulse, $t_0 = t_{add}$ if the dye is added after the pulse. As outlined in the text, the approximation $t_{obs} \rightarrow \infty$ applies.

In the limit of small membrane permeability, such that the exponential term in Eq. A8 is smaller than unity, the fraction of total dye uptake is given by

$$f(t_E) \approx \frac{P^0}{V_c} \cdot \int_{t_0}^{\infty} S_c(t_E, t) \cdot \mathrm{d}t \quad \text{(A9)}$$

Chemical kinetics of formation of electric pores

The concentration of pores in the state P_3 according to Eq. 12 is found by the solution of the system of the differential equations for the respective changes in the concentration of the pore states:

$$\frac{\mathrm{d}[C(t_E)]}{\mathrm{d}t_E} = -k_p \cdot [C(t_E)]$$

$$\frac{\mathrm{d}[P_1(t_E)]}{\mathrm{d}t_E} = -k_p \cdot ([P_1(t_E)] - [C(t_E)]) \quad \text{(10)}$$

$$\frac{\mathrm{d}[P_2(t_E)]}{\mathrm{d}t_E} = -k_p \cdot ([P_2(t_E)] - [P_1(t_E)])$$

$$\frac{\mathrm{d}[P_3(t_E)]}{\mathrm{d}t_E} = k_p \cdot [P_2(t_E)]$$

The boundary conditions of the integration are $[C(0)] = [P_0]$, $[P_{1,2,3}(0)] = 0$. Mass conservation dictates that the total number of membrane states is given by $[P_0] = [C(t_E)] + \Sigma_{i=1}^{3}[P_i(t_E)]$.

One key result we obtained was an analytical expression for the increase in the concentration of the dye-permeable pore state as a function of the pulse time:

$$[P_3(t_E)] = [P_o](1 - (1 + k_p t_E(1 + k_p t_E/2))\exp(-k_p t_E)) \quad \text{(A11)}$$

The total surface S of all electropores is here proportional to $[P_3]$ such that $[P_3]/[C_o] = S_c/S_c^o$, where S_c^o is the maximum value of S_c. Hence the time course of the build-up of the dye-permeable porated membrane surface S_c in the external electric field E is given by

$$S_c(t_E) = S_c^o \cdot \left[1 - \left(1 + k_p \cdot t_E \cdot \left(1 + \frac{k_p \cdot t_E}{2}\right)\right) \cdot e^{-k_p \cdot t_E}\right] \quad \text{(A12)}$$

The term S_c^o, similar to $[C_o]$, is independent of field duration and field strength, yet S_c^o is specific for every cell system (Neumann et al., 1996). Substitution of equation Eq. A12 in Eq. A9 yields Eq. 24.

Dye binding to the cell surface

The rate and extent of cell coloring also depend on the external dye concentration c. Here we may use the approximation $c \approx c_o = 1$ mM. The diffusion-limited dye binding rate $k_{ass} \cdot c$, where $k_{ass} = 10^8$ M^{-1} s^{-1} (Eigen and DeMayer, 1963), is therefore larger (10^5 s^{-1}) than the membrane transport rate ($k_f = 10^2$ s^{-1}). Hence the binding step Dy + (C $\rightleftharpoons$ P) $\rightleftharpoons$ Dy $\cdot$ (C $\rightleftharpoons$ P) in Eq. 9 can be considered as being rapidly equilibrated relative to the transport, and the flow coefficient takes the form

$$k_f = k_f^* \cdot f_b \quad \text{(A13)}$$

where k_f^* is the intrinsic coefficient for the transport step Dy $\cdot$ P $\rightleftharpoons$ P $\cdot$ Dy of the dye across the membrane, i.e., at saturated binding $f_b = 1$. The fraction of surface binding is given by the concentration ratio:

$$f_b = [\text{Dy} \cdot (\text{C} \rightleftharpoons \text{P})]/([\text{Dy} \cdot (\text{C} \rightleftharpoons \text{P})] + [\text{Dy}]) = \frac{c}{c + K_c} \quad \text{(A14)}$$

where $K_c = [\text{Dy}] \cdot [\text{C} \rightleftharpoons \text{P}]/[\text{Dy} \cdot (\text{C} \rightleftharpoons \text{P})]$ is the dissociation equilibrium constant of the binding step. Note that at saturation, $c \gg K_c$, hence $f_b \approx 1$. The term k_f^* is thus obtained from a dependence of k_f on $[\text{Dy}] = c$.

REFERENCES

Bradford, M. M. 1976. A rapid and sensitive method for the quantitation of microgram quantities of protein utilizing the principle of protein-dye binding. *Anal. Biochem.* 72:248–254.

Budde, P., N. Bewarder, V. Weinrich, and J. Frey. 1994. Biological functions of human FcγRIIa/FcγRIIc in B cells. *Eur. J. Cell Biol.* 64:45–60.

Dimitrov, D. S., and A. E. Sowers. 1990. Membrane electroporation—fast molecular exchange by electroosmosis. *Biochim. Biophys. Acta.* 1022: 381–392.

Domenge, C. S., B. Orlowski, T. Luboinski, G. De Baere, Jr., Schwaab, J. Belehradek, and L. M. Mir. 1996. Antitumor electrochemotherapy—new advances in the clinical protocol. *Cancer.* 77:956–963.

Eigen, M., and L. DeMayer. 1963. Relaxation methods. *In* Techniques of Organic Chemistry, Vol. 8. John Wiley, New York. 895–1054.

Evans, E. A. 1974. Bending resistance and chemically induced moments in membrane bilayers. *Biophys. J.* 14:923–931.

Gass, G. V., and L. V. Chernomordik. 1990. Reversible large scale deformations in the membranes of electrically-treated cells: electroinduced bleb formation. *Biochim. Biophys. Acta.* 1023:1–11.

Heller, R., and R. Gilbert. 1993. Development of electrically enhanced drug delivery procedures for the treatment of melanoma and pancreatic cancer. *In* Proceedings of the BES Symposium. Bielefeld University Press, Bielefeld, Germany. 10.

Heller, R., M. J. Jaroszeski, L. F. Glass, J. L. Messina, D. P. Rapaport, R. C. DeConti, N. A. Fenske, R. A. Gilbert, L. M. Mir, and D. S. Reintgen. 1996. Phase I/II trial for the treatment of cutaneous and subcutaneous tumors using electrochemotherapy. *Cancer.* 77:964–971.

Heller, R., M. J. Jaroszeski, J. Leo-Messian, R. Perrot, N. Van Voorhis, D. Reintgen, and R. Gilbert. 1995. Treatment of B16 mouse melanoma with the combination of electropermeabilization and chemotherapy. *Bioelectrochem. Bioenerg.* 36:83–87.

Hibino, M., H. Itoh, and K. Kinosita. 1993. Time courses of cell electroporation as revealed by submicrosecond imaging of transmembrane potential. *Biophys. J.* 64:1789–1800.

Hodgkin, A. L., and B. Katz. 1949. The effect of sodium ions on the electrical activity of the giant axon of the squid. *J. Physiol. (Lond.).* 108:37–77.

Israelachvili, J. N., and R. M. Pashley. 1984. Measurement of the hydrophobic interaction between two hydrophobic surfaces in aqueous electrolyte solutions. *J. Colloid Interface Sci.* 98:500–514.

Kakorin, S., S. P. Stoylov, and E. Neumann. 1996. Electro-optics of membrane electroporation in diphenylhexatriene-doped lipid bilayer vesicles. *Biophys. Chem.* 58:109–116.

Kinosita, K., Jr., and T. Y. Tsong. 1977. Formation and resealing of pores of controlled sizes in human erythrocyte membrane. *Nature.* 268: 438–441.

Kinosita, K., Jr., and T. Y. Tsong. 1978. Survival of sucrose-loaded erythrocytes in the circulation. *Nature.* 272:258–260.

McIntosh, T. J., and A. D. Magid. 1993. Phospholipid hydration. *In* Phospholipids Handbook. G. Cevc, editor. Marcel Dekker, New York. 553–578.

Mir, L. M., O. Tounekti, and S. Orlowski. 1996. Bleomycin: revival of an old drug. *Gen. Pharmacol.* 27:745–748.

Montane, M-H., E. Dupille, G. Alibert, and J. Teissie. 1990. Induction of a long-lived fusogenic state in viable plant protoplasts permeabilized by electric fields. *Biochim. Biophys. Acta.* 1024:203–207.

Neumann, E. 1989. The relaxation hysteresis of membrane electroporation. *In* Electroporation and Electrofusion in Cell Biology. E. Neumann, A. E. Sowers, and C. A. Jordan, editors. Plenum, New York. 61–82.

Neumann, E. 1992. Membrane electroporation and direct gene transfer. *Bioelectrochem. Bioenerg.* 28:247–267.

Neumann, E. 1996. Electric and magnetic field reception. *In* Encyclopedia of Molecular Biology and Molecular Medicine, Vol. 2. R. A. Meyers, editor. VCH, New York. 172–181.

Neumann, E., and E. Boldt. 1989. Membrane electroporation: biophysical and biotechnical aspects. *In* Charge and Field Effects in Biosystems, Vol. 2. M. H. Allen, S. F. Cleary, and F. M. Hawkridge, editors. Plenum, New York. 373–383.

Neumann, E., and E. Boldt. 1990. Membrane electroporation: the dye method to determine the cell membrane conductivity. *In* Horizons in Membrane Biotechnology. C. Nicolau, D. Chapman, and A. R. Liss, editors. Wiley-Liss, New York. 69–31.

Neumann, E., and S. Kakorin. 1996. Electrooptics of membrane electroporation and vesicle shape deformation. *Curr. Opin. Colloid Interface Sci.* 1:790–799.

Neumann, E., S. Kakorin, I. Tsoneva, B. Nikolova, and T. Tomov. 1996. Calcium-mediated DNA adsorption to yeast cells and kinetics of cell transformation. *Biophys. J.* 71:868–877.

Neumann, E., M. Schaefer-Ridder, Y. Wang, and P. H. Hofschneider. 1982. Gene transfer into mouse lyoma cells by electroporation in high electric fields. *EMBO J.* 1:841–845.

Parsegian, V. A. 1969. Energy of an ion crossing a low dielectric membrane: solutions to four relevant electrostatic problems. *Nature.* 221:844–846.

Pliquett, U., E. A. Gift, and J. C. Weaver. 1996. Determination of the electrical field and anomalous heating caused by exponential pulses with aluminum electrodes in electroporation experiments. *Bioelectrochem. Bioenerg.* 39:39–53.

Schwarz, G. 1967. On dielectric relaxation due to chemical rate processes. *J. Phys. Chem.* 71:4021–4030.

Seifert, U., and R. Lipowsky. 1995. Morphology of vesicles. *In* Structure and Dynamics of Membranes, Vol. 1A. R. Lipowsky and E. Sackmann, editors. Elsevier/North Holland, Amsterdam. 403–463.

Sersa, G., M. Gemazar, and D. Miklavcic. 1995. Antitumor effectiveness of electrochemo-therapy with *cis*-diamminedichloroplatinum (II) in mice. *Cancer Res.* 55:3450–4355.

Sowers, A. E. 1987. The long-lived fusogenic state induced in erythrocyte ghosts by electric pulses is not laterally mobile. *Biophys. J.* 52: 1015–1020.

Sowers, A. E., and M. R. Lieber. 1986. Electropore diameters, lifetime, numbers, and locations in individual erythrocyte ghosts. *FEBS Lett.* 205:179–184.

Teissie, J., and T. Y. Tsong. 1981. Electric field induced transient pores in phospholipid bilayer vesicles. *Biochemistry.* 20:1548–1554.

Tekle, E., R. D. Astumian, and P. B. Chock. 1990. Electro-permeabilization of cell membranes: effect of the resting membrane potential. *Biochem. Biophys. Res. Commun.* 172:282–287.

Tekle, E., R. D. Astumian, and P. B. Chock. 1991. Electroporation by using bipolar oscillating electric field: an improved method for DNA transfection of NIH 3T3 cells. *Proc. Natl. Acad. Sci. USA.* 8:4230–4234.

Tekle, E., R. D. Astumian, and P. B. Chock. 1994. Selective and asymmetric molecular transport across electroporated cell membranes. *Proc. Natl. Acad. Sci. USA.* 91:11512–11516.

Tsong, T. Y. 1991. Electroporation of cell membranes. *Biophys. J.* 60: 297–308.

Vanbever, R., and V. Preat. 1995. Factors affecting transdermal delivery of metoprolol by electroporation. *Bioelectrochem. Bioenerg.* 38:223–228.

Weaver, J. C., and Yu. A. Chizmadzhev. 1996. Theory of electroporation: a review. *Bioelectrochem. Bioenerg.* 41:135–160.